

Detecting Entanglement in Unfaithful States

Yongtao Zhan^{1,*} and Hoi-Kwong Lo^{1,2}

¹*Department of Electrical and Computer Engineering,
University of Toronto, Toronto, Ontario, M5S 3G4, Canada*

²*Department of Physics, University of Hong Kong, Pokfulam, Hong Kong*
(Dated: July 13, 2022)

Entanglement witness is an effective method to detect entanglement in unknown states without doing full tomography. One of the most widespread schemes of witnessing entanglement is measuring its fidelity with respect to a pure entangled state. Recently, a large class of states whose entanglement can not be detected with the fidelity witness has been discovered in Phys.Rev.Lett **124**,200502(2020). They are called unfaithful states. In this paper we propose a new way to detect entanglement by calculating the lower bound of entanglement using measurement results. Numerical simulation shows our method can detect entanglement in unfaithful states with a small number of measurements. Moreover, we generalize our scheme to multipartite states and show that it can tolerate higher noise than previous entanglement witness operators with same number of measurement settings.

I. INTRODUCTION

The concept of entanglement has played a crucial role in the development of quantum physics. The Einstein, Podolsky and Rosen effect[1] has received world-wide attention and has been a hot topic of research for decades. Entanglement has come to be recognized as a novel resource that may be used to perform tasks that are either impossible or very inefficient in the classical realm, for instance, Quantum Key Distribution(QKD)[2], quantum superdense coding[3], Quantum teleportation[4], quantum computing[5], etc. These developments have provided the seed for the development of modern quantum information science.

In an experiment we may prepare different kinds of quantum states. It is important for us to know whether a state prepared by us is entangled or not. A trivial way is performing full tomography of the state and it requires a large amount of measurements. Take a N -qubit state as an example, we need 2^{2N} measurements to determine all matrix elements of the density matrix ρ . So, the number of measurements grows exponentially with the particle number N . *Entanglement witness* is an efficient scheme to detect entanglement in an unknown state and it requires a much smaller number of measurements compared to full tomography[6]. As shown in Figure.1, the set of separable states is a convex subset in the Hilbert space. The Hahn-Banach theorem guarantees that there exists a hyperplane for every entangled state ρ that separates this state from the separable set. These hyperplanes correspond to observables W , such that $\text{Tr}(W\rho) < 0$, whereas $\text{Tr}(W\sigma) \geq 0$ for all separable states σ . If the measured value $\langle W \rangle_\rho$ is positive, we can not tell whether the state is entangled or not. However, we can know for sure that ρ_{exp} is an entangled state if the measurement produces a negative expectation value. Such observable W is called entanglement witness oper-

ator. Although W exists for each entangled state ρ , it is formidable to construct a useful witness operator without specific information about the state produced in the experiment.

However, when the underlying state is expected to be close to a target entangled state $|\psi\rangle$, entanglement witness can be done by measuring the fidelity between the two states. This is called the fidelity witness. Fidelity witness has been widely studied both theoretically and experimentally[7–15].

Unfortunately, a recent paper shows that fidelity witness is severely limited in its ability in detecting entanglement and, in fact, a large class of entangled states, called *unfaithful states*, cannot be detected by fidelity witness[16]. For high dimensional systems($d > 2$), they find, surprisingly, that almost no bipartite entangled state can be detected using fidelity witness. Their work is a warning toward the blind application of fidelity-type entanglement witnesses. And it shows the importance of detecting entanglement in unfaithful states.

In this paper we present a new scheme of generalized entanglement witness, which can detect entanglement in unfaithful states. Our scheme is summarized as follows: We measure a set of Hermitian operators A_1, A_2, \dots, A_n in experiment and use the measured values a_1, a_2, \dots, a_n to calculate the lower bound of entanglement of the state ρ

$$\varepsilon(a_1, \dots, a_n) = \inf_{\rho} \{E(\rho) \mid \text{Tr}(\rho A_k) = a_k\} \quad (1)$$

where $E(\rho)$ is certain entanglement measure and the infimum is understood as the infimum over all states compatible with the data $a_k = \text{Tr}(A_k \rho)$. In this paper, we choose $E(\rho)$ to be geometric measure of entanglement E_G for bipartite states. The geometric measure E_G is positive only when a bipartite state is entangled. If we get a positive value of the lower bound of entanglement $\varepsilon(a_1, \dots, a_n)$, we can know for sure that the state is entangled. On the other hand, if the lower bound is zero, we cannot tell whether a state is entangled or not. Our

* yongtao.zhan@mail.utoronto.ca

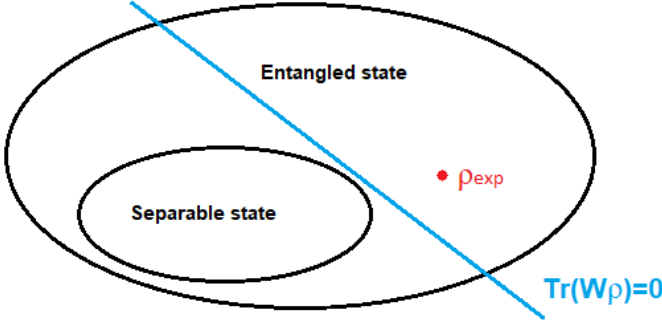


FIG. 1. The Venn diagram of the Hilbert space. The separable states forms a convex set and the equation $Tr(W\rho) = 0$ is a hyperplane in Hilbert space. ρ_{exp} is the state we prepare in the experiment. For the upper part of the Hilbert space, $Tr(W\rho)$ is negative and for the lower part, it is positive. If we get a negative expectation value in the experiment, we know ρ_{exp} is an entangled state.

scheme can successfully detect entanglement in unfaithful states.

Furthermore, our scheme can be extended to the case of multipartite stabilizer states (e.g. cluster states) and non-stabilizer states (e.g. W state). In order to detect genuine entanglement in multipartite states, the entanglement measure $E(\rho)$ is chosen to be the generalized geometric measure (GGM) [17, 18]. The GGM is positive only when the state is genuinely entangled. So if the lower bound of GGM of state ρ is positive, the state must carry genuine multipartite entanglement. We find our scheme can tolerate higher noise than the previously constructed witness operators [8, 9, 19, 20] while using the same number of measurement settings.

Although there are nonlinear witnesses which also can detect entanglement in unfaithful states [21–24], they usually take more measurements. Moreover, they can only be applied to bipartite systems, which means they can not be generalized to detect genuine entanglement in multipartite states [20].

Our paper is organized as follows: we review the fidelity witness and the main conclusions about unfaithful state in Ref. [16] in Section II. The theory and numerical algorithms of calculating the lower bound of entanglement is discussed in Section III and Section IV. We show how to detect entanglement in bipartite unfaithful state in Section V. In Section VI and Section VII, we extend our scheme to the case of multipartite cluster state and non-stabilizer states.

II. ENTANGLEMENT WITNESS AND UNFAITHFUL STATES

Definition 1. An N -qudit pure state $|\Psi\rangle$ is fully separable iff it can be written as

$$|\Psi\rangle = \bigotimes_{i=1}^m |\Psi_{A_i}\rangle \quad (2)$$

where $|\Psi_{A_i}\rangle$ is the state of the i -th qudit.

An N -qudit mixed state ρ_s is fully separable iff it can be decomposed into convex mixture of fully separable pure states

$$\rho_s = \sum_i p_i |\Psi_i\rangle\langle\Psi_i| \quad (3)$$

Definition 2. An N -qudit pure state $|\Psi\rangle$ is biseparable iff there exists a subsystem bipartition $\{A, \bar{A}\}$, where \bar{A} is the complement of set A , the state can be written as

$$|\Psi\rangle = |\Psi_A\rangle \otimes |\Psi_{\bar{A}}\rangle \quad (4)$$

An N -qudit mixed state ρ_s is biseparable iff it can be decomposed into convex mixture of biseparable pure states

$$\rho_s = \sum_i p_i |\Psi_i\rangle\langle\Psi_i| \quad (5)$$

Definition 3. An N -qudit mixed state ρ is said to be *genuine entangled* (or carrying genuine multipartite entanglement) iff it is not a biseparable state.

Definition 4. A fidelity witness operator that detects genuine entanglement of a pure state $|\psi\rangle$ (and of states that are close to $|\psi\rangle$) is given by [7]

$$\mathcal{W} = \alpha \mathbb{I} - |\psi\rangle\langle\psi| \quad (6)$$

The constant α denotes the maximum overlap between the state $|\psi\rangle$ and any biseparable state $|\phi\rangle$.

$$\alpha = \max_{|\phi\rangle \in B} |\langle\phi|\psi\rangle|^2 \quad (7)$$

where B denotes the set for biseparable state. It is clear that $Tr(\mathcal{W}\rho) > 0$ for any biseparable state ρ . On the contrary, we know for sure that ρ carries genuine multipartite entanglement if we obtain negative expectation value. The witness operator in Eq. (6) is called the fidelity witness because it involves measuring the fidelity between the state ρ and $|\psi\rangle$.

In Ref. [7], the authors implement the witness operator in Eq. (6) experimentally to detect entanglement in three-qubit W state and GHZ state. In order to measure it in the experiment, it must be decomposed into sum of locally measurable operators [25]. Despite its compact mathematical form, the fidelity witness is difficult to implement in large systems because the number of measurements grows exponentially with the number of

d	$\mathcal{S}^1(HS)$	$\tilde{\mathcal{U}}_2 \setminus \mathcal{S}^1(HS)$	$\mathcal{S}^1(B)$	$\tilde{\mathcal{U}}_2 \setminus \mathcal{S}^1(B)$
2	24.3 %	58.5 %	24.2 %	21.1 %
3	0.01 %	99.9 %	0.01 %	94.5 %
4	0 %	100 %	0 %	99.9 %
5	0 %	100 %	0 %	100 %

TABLE I. The lower bound of percentage of bipartite separable state (\mathcal{S}^1) and unfaithful state ($\tilde{\mathcal{U}}_2 \setminus \mathcal{S}^1$) in whole Hilbert space in small dimensions. This table is reproduced from TABLE I in Ref.[16]. The percentage are calculated in Hilbert-Schmidt metric and Bures metric. It is obvious that for $d > 2$, most state in Hilbert space are both entangled and unfaithful.

qubits[7, 26]. So it is only feasible in small systems.

In order to solve this problem, a large class of witness operator called *fidelity-type witness* has been derived[9, 20]. A fidelity-type witness \mathcal{W}' is constructed using the following inequality

$$\mathcal{W}' - \alpha \mathcal{W} \geq 0 \quad (8)$$

which means $\mathcal{W}' - \alpha \mathcal{W}$ is a semi-definite matrix and α is certain positive number. Thus the witness operator \mathcal{W}' can detect entanglement ($\text{Tr}(\mathcal{W}'\rho) < 0$) only when the fidelity witness can ($\text{Tr}(\mathcal{W}\rho) < 0$). Although the fidelity-type witness \mathcal{W}' can not detect as many entangled states as the fidelity witness \mathcal{W} , it can be implemented with fewer measurements. For example, in Ref.[9], the authors constructed fidelity-type witnesses for cluster states and GHZ states, which can be implemented using two measurement settings.

Recently, researchers find a large class of states whose entanglement can not be detected using any fidelity witnesses (thus can not be detected using any fidelity-type witnesses either)[16]. They call them *unfaithful states*. They use \mathcal{S} to denote the set of separable states and \mathcal{U}_2 to denote the set of states that satisfied $\text{Tr}(\mathcal{W}\rho) \geq 0$ for any fidelity witness \mathcal{W} . In order to find the percentage of the set of bipartite unfaithful state $\mathcal{U}_2 \setminus \mathcal{S}$ in the whole Hilbert space, they use a semidefinite programming (SDP) ansatz. The set \mathcal{S}^1 and $\tilde{\mathcal{U}}_2 \setminus \mathcal{S}^1$ are the outer approximations of the set separable state \mathcal{S} and $\mathcal{U}_2 \setminus \mathcal{S}$. The percentages are calculated by sampling random bipartite state according to Hilbert-Schmidt measure[27, 28] and Bures measure[29]. The lower bound of the percentage of separable state and unfaithful state in the whole Hilbert space is shown in Table I. We can easily find for $d \geq 3$, almost all states in the Hilbert space are unfaithful. From $d > 5$ on, the authors find that all states they generated are entangled but at the same time unfaithful, regardless of whether they sample according to the Hilbert-Schmidt or the Bures metric. This highlights the importance of characterizing the entanglement of unfaithful qudit states beyond relying on fidelity witnesses.

The authors also find most pure entangled state re-

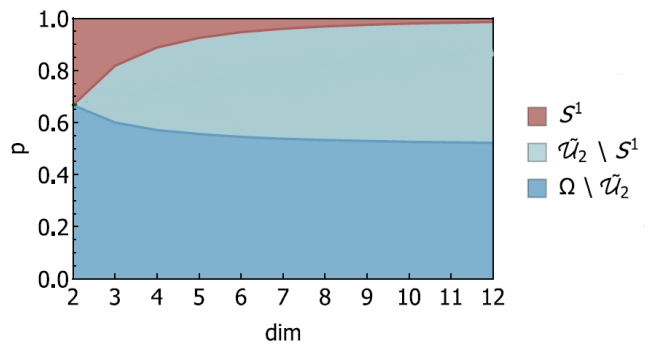


FIG. 2. The graph of unfaithful and entangled region of the family of state ρ from Eq.(9). This figure is reproduced from FIG.2 in Ref.[16]. The red region indicated the set of separable states. The green region indicates the set of unfaithful and entangled states. The blue region indicates the set of faithful states, whose entanglement can be detected using fidelity witness.

mained entangled but become unfaithful when a certain amount of white noise is added. Consider the Bell state $|\Psi_2\rangle = (|00\rangle + |11\rangle)/\sqrt{2}$ embedded in $d \times d$ Hilbert space.

$$\rho = p \frac{\mathbb{I}}{d^2} + (1-p)|\Psi_2\rangle\langle\Psi_2| \quad (9)$$

It is easy to prepare such a state by drawing a random state from either a completely mixed state or the state $|\Psi_2\rangle$ with a probability p and $1-p$ respectively. For $d > 2$, there exists a large parameter regime where the state ρ is entangled and unfaithful. This phenomenon is shown in Fig.2. What's more, they find numerically that all sampled pure entangled state are unfaithful and entangled for a certain range of white noise. The only exception they find is the maximally entangled state $1/\sqrt{d} \sum_{i=0}^{d-1} |ii\rangle$ subjected to white noise.

III. QUANTIFYING ENTANGLEMENT WITH SIMPLE MEASUREMENTS

In Ref.[30, 31], the authors present a method to estimate the entanglement with the measured expectation value of witness operators. In this section we briefly summarize their results.

Suppose we measure n witness operators $\{\mathcal{W}_1, \mathcal{W}_2, \dots, \mathcal{W}_n\}$ on the state in the experiment and their expectation values are w_1, w_2, \dots, w_n . We hope to find the lower bound of entanglement based on our measurement results.

$$\varepsilon(w_1, \dots, w_n) = \inf_{\rho} \{E(\rho) \mid \text{Tr}(\rho \mathcal{W}_k) = w_k\} \quad (10)$$

where the infimum is understood as the infimum over all states compatible with the measurement data. We note that $\varepsilon(w_1, \dots, w_n)$ is a convex function. The proof of this is simple and will be presented in the appendix. We

consider linear bounds of the type

$$\varepsilon(w) \geq r \cdot w - c \quad (11)$$

Note r and w are both n -dimensional vectors and the dot denotes dot product in this inequality. For one dimensional case, the two bounds are plotted in Figure.3. Intending to find the best estimation of the entanglement lower bound $\varepsilon(w)$, the intercept c should be as small as possible. By the definition of $\varepsilon(w)$, we note that Eq.(11) can be expressed as $E(\rho) \geq r \cdot w - c$. So we arrive at the inequality of c .

$$c \geq \sum_k r_k \text{Tr}(\rho \mathcal{W}_k) - E(\rho) \quad (12)$$

This indicates that we should perform maximization over the whole state space and choose c to be the supremum of the right hand side(RHS), which only depends on the operator $\mathcal{W} = \sum_k r_k \mathcal{W}_k$. Thus the supremum of the RHS can be expressed as the function $\hat{E}(\mathcal{W})$, which is

$$\hat{E}(\mathcal{W}) = \sup_{\rho} \{\text{Tr}(\rho \mathcal{W}) - E(\rho)\} \quad (13)$$

After getting the minimum value of c , we vary the slope r to arrive at the best possible bound $\varepsilon(w)$, as we have shown in Figure.3.

$$\varepsilon(w) = \sup_r \left\{ \sum_k r_k w_k - \hat{E} \left(\sum_k r_k \mathcal{W}_k \right) \right\} \quad (14)$$

Note Eq.(14) is a Legendre transform formula. That means $\varepsilon(w)$ is the Legendre transformation of the function $\hat{E}(r) = \hat{E}(\sum_k r_k \mathcal{W}_k)$.

The entanglement measure $E(\rho)$ is often defined through the convex roof construction[32]

$$E(\rho) = \min_{p_i, |\psi_i\rangle} \left\{ \sum_i p_i f(|\psi_i\rangle) : \sum_i p_i |\psi_i\rangle \langle \psi_i| = \rho \right\} \quad (15)$$

where f can be chosen as the geometric measure of entanglement, entanglement of formation, etc. In this way the function $\hat{E}(\mathcal{W})$ can be evaluated by:

$$\begin{aligned} \hat{E}(\mathcal{W}) &= \sup_{\rho} \left\{ \text{Tr}(\rho \mathcal{W}) - \inf_{p_i, |\psi_i\rangle} \sum_i p_i E(|\psi_i\rangle) \right\} \\ &= \sup_{p_i} \sup_{|\psi_i\rangle} \left\{ \sum_i p_i \{ \langle \psi_i | \mathcal{W} | \psi_i \rangle - E(|\psi_i\rangle) \} \right\} \\ &= \sup_{|\psi\rangle} \{ \langle \psi | \mathcal{W} | \psi \rangle - E(|\psi\rangle) \} \end{aligned} \quad (16)$$

Thus the process of calculating the lower bound can be summarized as follows: First we choose what kind of entanglement measure to use and calculate minimum value of intercept c . Then we do the optimization over the slope r according to Eq.(14) to get the lower bound of

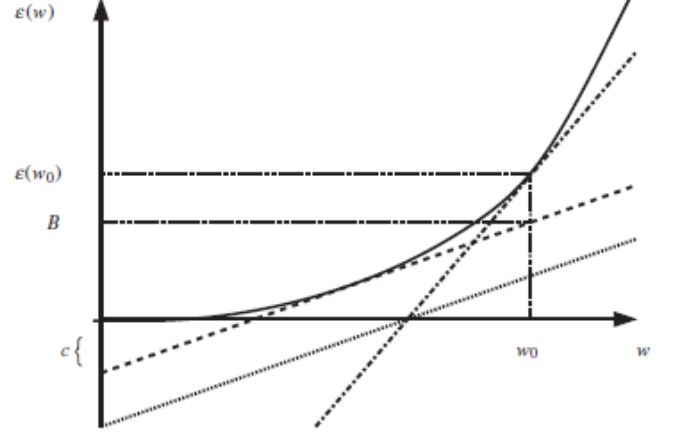


FIG. 3. A schematic view of the estimation method. This figure is reproduced from Ref.[30]. The lower bound $\varepsilon(w)$ is a convex function. We assume that w_0 is the measured expectation value. The dotted line correspond to a general estimation. First we perform the minimization on the intercept c and the linear bound becomes the dashed line. We can get a better estimation of the entanglement lower bound, which is B . By varying the slope r we arrive at the dash-dotted line, which gives the best estimation of the lower bound $\varepsilon(w_0)$.

entanglement $E(\rho)$.

IV. CALCULATING THE LOWER BOUND OF GEOMETRIC MEASURE AND GENERALIZED GEOMETRIC MEASURE

In this section we generalize the scheme in previous section to calculating the lower bound of entanglement with measurement results of any Hermitian operators, instead of witness operators. Moreover, we show the numerical calculation of lower bound of entanglement with a set of measured values.

We measure a set of Hermitian operators A_1, A_2, \dots, A_n in experiment and use the measured values a_1, a_2, \dots, a_n to calculate the lower bound of entanglement of the state ρ

$$\varepsilon(a_1, \dots, a_n) = \inf_{\rho} \{E(\rho) \mid \text{Tr}(\rho A_k) = a_k\} \quad (17)$$

Simply replacing the witness operators $\{\mathcal{W}_1, \mathcal{W}_2, \dots, \mathcal{W}_n\}$ in Eq.(10) with Hermitian operators $\{A_1, A_2, \dots, A_n\}$, the lower bound $\varepsilon(a_1, a_2, \dots, a_n)$ can be calculated using the scheme summarized in Section.III. In this case, the maximum intercept in Eq.(13) can be rewrite as

$$\hat{E}(\mathcal{A}) = \sup_{\rho} \{\text{Tr}(\rho \mathcal{A}) - E(\rho)\} \quad (18)$$

where $\mathcal{A} = \sum_k r_k A_k$. If the entanglement measure is defined through the convex roof construction, $\hat{E}(\mathcal{A})$ can

be evaluated using

$$\hat{E}(\mathcal{A}) = \sup_{|\psi\rangle} \{ \langle \psi | \mathcal{A} | \psi \rangle - E(|\psi\rangle) \} \quad (19)$$

Finally, the lower bound $\varepsilon(a_1, a_2, \dots, a_n)$ can be calculated using

$$\varepsilon(a_1, a_2, \dots, a_n) = \sup_r \left\{ \sum_k r_k a_k - \hat{E} \left(\sum_k r_k A_k \right) \right\} \quad (20)$$

which is a modified version of Eq.(14)

The first problem of numerical calculation is what kind of entanglement measure $E(\rho)$ we should use. For extending to multipartite cases, the entanglement measure must be able to quantify multipartite entanglement. There are lots of multipartite entanglement measures including Schmidt measure, relative entanglement of entropy(REE), geometric measure[33]. Although the Schmidt measure is widely used in theoretical analysis of the entanglement of cluster state, it is not robust to noise, i.e. it may varies a lot if there is any small deviation in the quantum state. For relative entanglement of entropy, it is not constructed through the convex roof construction, and that make $E(\mathcal{A})$ hard to evaluate.

In Ref.[30], the authors show the calculation of lower bound of Entanglement of Formation(EoF) and geometric measure. In this paper, we use the geometric measure as a measure of bipartite entanglement. The geometric measure is an entanglement monotone[34] and is relatively easy to calculate[35, 36]. For pure states, the geometric measure is defined by

$$E_G(|\psi\rangle) = 1 - \sup_{|\phi\rangle=|a\rangle|b\rangle|c\rangle\cdots} |\langle \phi | \psi \rangle|^2 \quad (21)$$

as one minus the maximal squared overlap with separable states. For mixed states, the geometric measure of entanglement is defined via the convex roof construction in Eq.(15). By replacing the $E(|\psi\rangle)$ term in Eq.(19) with the geometric measure we get $\hat{E}_G(\mathcal{A})$ for bipartite states

$$\hat{E}_G(\mathcal{A}) = \sup_{|\psi\rangle} \sup_{|\phi\rangle=|a\rangle|b\rangle} \{ \langle \psi | (\mathcal{A} + |\phi\rangle\langle\phi|) | \psi \rangle - 1 \} \quad (22)$$

This function $\hat{E}_G(\mathcal{A})$ can be evaluated by doing optimization over all biseparable state $|\phi\rangle = |a\rangle|b\rangle$. After that, the entanglement lower bound $\varepsilon(a_1, a_2, \dots, a_n)$ can be calculated by optimizing the slope r using Eq.(20). The numerical algorithm for the optimization is presented in the appendix. By calculating the lower bound of entanglement, we can determine whether the bipartite state is entangled or not.

However, things become different when detecting genuine entanglement in multipartite states. The geometric measure of a multipartite state is positive if the state is not fully separable. So obtaining a positive lower bound does not means the state carries genuine entanglement. Here we use another kind of entanglement measure, the

generalized geometric measure(GGM)[17, 18]. The GGM of a pure state $|\psi\rangle$ is defined by

$$E_{GGM}(|\psi\rangle) = 1 - \sup_{|\phi\rangle=|\phi_A\rangle|\phi_{\bar{A}}\rangle} |\langle \phi | \psi \rangle|^2 \quad (23)$$

where the optimization is done over all biseparable states $|\phi\rangle$. An equivalent form of the equation is

$$E_{GGM}(|\psi\rangle) = 1 - \max_{A:\bar{A}} \lambda_{A:\bar{A}}^2 \quad (24)$$

where $\lambda_{A:\bar{A}}$ is the maximal Schmidt coefficient for any bipartite split $A : \bar{A}$ of the state $|\psi\rangle$. For mixed states, E_{GGM} is constructed using the convex-roof construction. It is obvious that E_{GGM} is positive iff the state carries genuine entanglement. The calculation of lower bound of E_{GGM} is similar to that of E_G , as we only have to change the optimization zone from full separable states to biseparable states. If we get a positive value for the lower bound of E_{GGM} , we can know the state is a genuine entangled state.

V. DETECTING ENTANGLEMENT IN BIPARTITE UNFAITHFUL STATES

In this section we give an example about applying our new scheme to detect entanglement in bipartite unfaithful state. For the convenience of comparison, we take the Bell state embedded in a $d \times d$ Hilbert space(Eq.(9)) as an example. We use three measurements $X \otimes X, Y \otimes Y$ and $Z \otimes Z$ to estimate the lower bound of entanglement of the state. The operators X, Y and Z are as follows:

$$X = \left[\begin{array}{cc|c} 0 & 1 & \\ 1 & 0 & \\ \hline & & 0 \end{array} \right]$$

$$Y = \left[\begin{array}{cc|c} 0 & -i & \\ i & 0 & \\ \hline & & 0 \end{array} \right]$$

$$Z = \left[\begin{array}{cc|c} 1 & 0 & \\ 0 & -1 & \\ \hline & & 0 \end{array} \right]$$

They are the Pauli operators in the subspace spanned by $|0\rangle$ and $|1\rangle$. The Pauli operators in subspace are easy to measure in experiment. For example, for qubits encoded in photon paths, we just have to measure the first and second path for obtain the outcomes $X \otimes X, Y \otimes Y, Z \otimes Z$. It is easy to check that $X \otimes X, Y \otimes Y$ and $Z \otimes Z$ are stabilizers of $|\Psi_2\rangle$. We use the measured values of the three stabilizers to calculate the lower

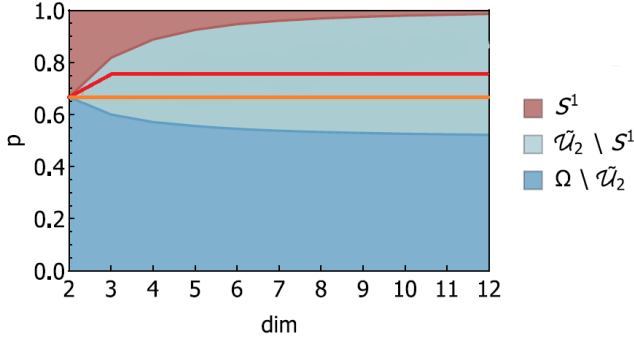


FIG. 4. The noise tolerance of fidelity witness and our method. The blue line is the bound of noise tolerance of any fidelity witness. The orange line is the noise tolerance of our method using only three measurements $X \otimes X, Y \otimes Y, Z \otimes Z$. If we add one more measurement $M \otimes M$, the noise tolerance is higher, which is depicted by the orange line. Our scheme achieves a big improvement over the fidelity witness.

bound of geometric entanglement. For the the state $\rho = p\mathbb{I}/d^2 + (1-p)|\Psi_2\rangle\langle\Psi_2|$, the measured values are $\langle X \otimes X \rangle = \langle Y \otimes Y \rangle = \langle Z \otimes Z \rangle = 1 - p$. For any dimension d , the entanglement lower bound is positive when $p < 2/3$, which we can know for sure that the state is entangled. For $p > 2/3$, the lower bound is zero, which we can not tell whether the state is entangled or not. So the noise tolerance of our method is $p = 2/3$.

We can add more measurements to give a better estimation of the lower bound of entanglement. This may detect the entanglement better. For example, the measurement $M \otimes M$ can be added when $d \geq 3$. The operator M reads:

$$M = \left[\begin{array}{ccc|c} 1 & 0 & 0 & \\ 0 & 0 & 0 & \\ 0 & 0 & -1 & \\ \hline & & & 0 \end{array} \right]$$

which is a Pauli-Z operator in the subspace spanned by $|0\rangle$ and $|2\rangle$. Hence we use four measurement results $\langle X \otimes X \rangle, \langle Y \otimes Y \rangle, \langle Z \otimes Z \rangle$ and $\langle M \otimes M \rangle$ to calculate the lower bound of entanglement. For any dimensions larger than 2, the lower bound is positive when $p < 3/4$. So the noise tolerance of our method is $p = 3/4$ with four measurements.

The numerical results are shown in Fig.4. As we have explained in Section II, the blue line is the noise tolerance bound of any fidelity witnesses. The orange line is the noise tolerance bound when three measurements $X \otimes X, Y \otimes Y, Z \otimes Z$ are used to detect entanglement. When we add one more measurement $M \otimes M$ for $d \geq 3$, the noise tolerance bound becomes higher, which is shown by the red line. If we use more measurements, the noise tolerance can be higher. As a conclusion, our method can be useful to detect entanglement in bipartite unfaithful states.



FIG. 5. An N -partite linear cluster state.

VI. DETECTING ENTANGLEMENT IN CLUSTER STATES

In this section we show our scheme can be used to detect genuine entanglement in cluster states. Using the same number of measurement settings, our scheme can tolerate higher noise than traditional witness operators, which can be useful for verifying genuine entanglement in cluster state experiments.

Cluster state is a type of highly entangled state of multiple qubits. It was first introduced in [37]. One important application of cluster state was used to be a resource state in the measurement-based computation, which was proposed in Ref.[38]. The cluster state has been carefully studied during the past two decades. Experimentalists have also tried to realize cluster state for the ultimate goal of measurement-based quantum computation[13, 39, 40].

An N -partite, d -level linear cluster state $|\phi_{N,d}\rangle$ is shown in Fig.5. It is uniquely defined by the eigenvalue equations

$$X_a \bigotimes_{b \in \mathcal{N}(a)} Z_b |\phi_{N,d}\rangle = |\phi_{N,d}\rangle \quad (25)$$

where

$$\mathcal{N}(a) = \begin{cases} \{2\}, & a = 1 \\ \{N-1\}, & a = N \\ \{a-1, a+1\}, & a \notin \{1, N\} \end{cases} \quad (26)$$

The X and Z are generalized Pauli matrices, which are introduced in Ref.[41]. In the stabilizer formalism, the N stabilizer generators are $\mathcal{S}_k = X_a \bigotimes Z_b$, where $k = 1, \dots, N$.

For measurement-based quantum computing, a large-scale cluster state is needed. So the problem of detecting genuine multipartite entanglement in cluster states becomes important. Two witness operators are presented in [8, 9] to solve the problem for linear cluster states.

$$\mathcal{W}_1 := 3\mathbb{I} - 2 \left[\prod_{\text{even } k} \frac{S_k + \mathbb{I}}{2} + \prod_{\text{odd } k} \frac{S_k + \mathbb{I}}{2} \right] \quad (27)$$

$$\mathcal{W}_2 := (N-1)\mathbb{I} - \sum_{k=1}^N S_k \quad (28)$$

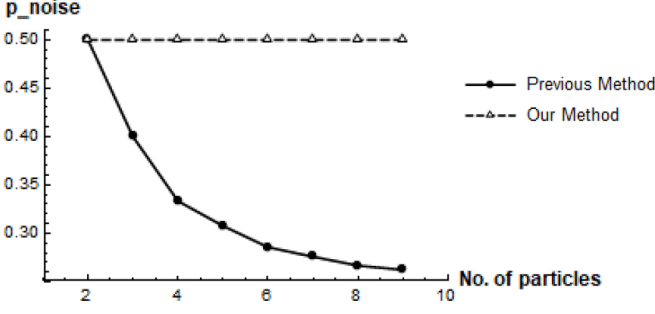


FIG. 6. The noise tolerance of our method and the witness operator \mathcal{W}_1 in N -qubit cluster states. The horizontal axis is the number of the particle and the vertical axis is the noise tolerance. The noise tolerance of our method is about 0.5 for any number of particle, while the noise tolerance of \mathcal{W}_1 , which is the best witness operator that has ever been derived, is close to 0.25 for large number of particles.

where S_k refers to the k -th stabilizer generator. Note the two witness operators are for cluster states of 2-level, i.e. qubits. These witness operators are robust against noise and require only two local measurement settings when used in an experiment, independent of the number of qubits, which is a big progress compared to the fidelity witness operator in Eq.(6). The witness operator \mathcal{W}_1 can tolerate higher noise than \mathcal{W}_2 . When the cluster state $|\phi_{N,2}\rangle$ is mixed with certain amount of white noise, the mixed state is

$$\rho = p_{noise} \mathbb{I}/2^N + (1 - p_{noise}) |\phi_{N,2}\rangle \langle \phi_{N,2}| \quad (29)$$

The noise tolerance of \mathcal{W}_1 reads

$$p_{noise} = \begin{cases} (4 - 4/2^{N/2})^{-1} & \text{for even } N \\ [4 - 2(1/2^{(N+1)/2} + 1/2^{(N-1)/2})]^{-1} & \text{for odd } N \end{cases} \quad (30)$$

, which is plotted in Fig.6 using blue points. For large N , the noise tolerance is close to 0.25.

We find our method can achieve a big improvement over the result in Eq.(27). By measuring all stabilizer generators S_1, S_2, \dots, S_N of the cluster state, our method requires the same number of measurement settings as the witness operator \mathcal{W}_1 .

We use N measured values to calculate the lower bound of generalized geometric measure (GGM). For the cluster state mixed with certain amount of white noise, the measurement results of the stabilizer generators are $\langle S_1 \rangle = \langle S_2 \rangle = \dots = \langle S_n \rangle = 1 - p_{noise}$. We find the lower bound of GGM is positive when $p_{noise} < 0.5$ for all particle number N . Our results is plotted in Fig.5 using orange points. It is obvious that our method can tolerate higher noise than the witness operator \mathcal{W}_1 .

VII. DETECTING ENTANGLEMENT IN NON-STABILIZER STATES

Similar ideas can be used for detection of entanglement of non-stabilizer state. For such states it is not possible to find 2^N operators such that they stabilize the state and also they are the tensor-products of single-qubit operators. For example, the three-qubit W -state $|W_3\rangle = (|001\rangle + |010\rangle + |100\rangle)/\sqrt{3}$ is a non-stabilizer state. If non-local operators are considered, the $|W_3\rangle$ state is stabilized by [9]

$$\begin{aligned} S_1^{(W_3)} &:= -\frac{1}{3}(ZZI - 2XXI - 2YIY) \\ S_2^{(W_3)} &:= -\frac{1}{3}(IZZ - 2IXX - 2YYI) \\ S_3^{(W_3)} &:= -\frac{1}{3}(ZIZ - 2XIX - 2IYY) \end{aligned} \quad (31)$$

There is only a single state, the $|W_3\rangle$ state, that gives +1 for all the three operators. A witness operator detecting genuine three-qubit entanglement around a $|W_3\rangle$ state with only three measurement settings is constructed in Ref.[9], which reads

$$\mathcal{W}_w = \frac{11}{3} \mathbb{I} + 2Z_1 Z_2 Z_3 - \frac{1}{3} \sum_{k \neq l} (2X_k X_l + 2Y_k Y_l - Z_k Z_l) \quad (32)$$

For the $|W_3\rangle$ state mixed with certain amount of white noise $\rho = p_{noise} \mathbb{I}/8 + (1 - p_{noise}) |W_3\rangle \langle W_3|$, the witness operator \mathcal{W}_w tolerates noise if $p_{noise} < 4/15 \approx 0.27$.

In our new scheme, we choose to measure three non-local stabilizers in Eq.(31), which also requires three measurement settings XXX , YYY and ZZZ . The three measurement results can be used to calculate the lower bound of generalized geometric measure. For the $|W_3\rangle$ state mixing with certain amount of white noise, the measurement results of the stabilizer generators are $\langle S_1^{(W_3)} \rangle = \langle S_2^{(W_3)} \rangle = \langle S_3^{(W_3)} \rangle = 1 - p_{noise}$. According to our numerical calculation, the lower bound of GGM is positive if $p_{noise} < 0.45$. Thus our scheme can detect genuine entanglement when $p_{noise} < 0.45$, which achieves an improvement over the witness operator \mathcal{W}_w with same number of measurement settings.

VIII. APPLICATION IN EXPERIMENT

In this section, we apply our new scheme of detecting entanglement to previous cluster state experiment.

In Ref.[42], the authors prepared a four-qubit cluster state and measured the stabilizer generators. The measurement outcomes are shown in Table.II. Using their experimental data, we can calculate the lower bound of GGM, which is $\varepsilon_{GGM} = 0.170 \pm 0.004$ for the four-qubit state. Obtaining positive values of the lower bound means the state prepared in experiment are genuine entangled.

Although our scheme and previous witness operators can detect genuine entanglement in this case, our method

Generators	Measurement outcomes
$g_1 = -Z_1 \otimes Z_2 \otimes \mathbb{I}_3 \otimes \mathbb{I}_4$	0.994 ± 0.001
$g_2 = -X_1 \otimes X_2 \otimes Z_3 \otimes \mathbb{I}_4$	0.849 ± 0.003
$g_3 = \mathbb{I}_1 \otimes Z_2 \otimes X_3 \otimes X_4$	0.937 ± 0.003
$g_4 = \mathbb{I}_1 \otimes \mathbb{I}_2 \otimes Z_3 \otimes Z_4$	0.911 ± 0.002

TABLE II. Four-qubit cluster state: measurement outcomes of stabilizer generators. This table is reproduced from Table.1 in Ref.[42]

can tolerate higher noise. Take the four-qubit cluster state mixed with white noise for example. If $p_{noise} \approx 0.4$, i.e. $\langle g_1 \rangle = \langle g_2 \rangle = \langle g_3 \rangle = \langle g_4 \rangle \approx 0.6$, the witness operator \mathcal{W}_1 will give a positive expectation value, which can not detect genuine entanglement, while our method give a lower bound of GGM $\varepsilon_{GGM} \approx 0.1$, which can detect genuine entanglement in the presence of high noise.

IX. CONCLUSION

In this paper we proposed a new way of entanglement witness, which can detect entanglement in unfaithful state. Furthermore we extend it to the case of multi-particle states. We show our scheme can tolerate higher noise than previous witness operators, while using the same number of measurement settings. Our scheme can be useful for detecting entanglement in experimentally prepared states.

X. ACKNOWLEDGEMENT

We thank discussions and comments from Ilan Tzitrin. We thank funding support from NSERC, CFI, ORF, Huawei Technologies Canada, MITACS, US Office of Naval Research, Royal Bank of Canada and the University of Hong Kong start-up grant.

-
- [1] A. Einstein, B. Podolsky, and N. Rosen, Phys. Rev. **47**, 777 (1935).
 - [2] F. Xu, X. Ma, Q. Zhang, H.-K. Lo, and J.-W. Pan, Rev. Mod. Phys. **92**, 025002 (2020).
 - [3] C. H. Bennett and S. J. Wiesner, Phys. Rev. Lett. **69**, 2881 (1992).
 - [4] C. H. Bennett, G. Brassard, C. Crépau, R. Jozsa, A. Peres, and W. K. Wootters, Phys. Rev. Lett. **70**, 1895 (1993).
 - [5] R. Raussendorf, D. E. Browne, and H. J. Briegel, Phys. Rev. A **68**, 022312 (2003).
 - [6] M. M. Nicolai Friis, Giuseppe Vitagliano and M. Huber, Nature Review Physics **1**, 72 (2019).
 - [7] M. Bourennane, M. Eibl, C. Kurtsiefer, S. Gaertner, H. Weinfurter, O. Gühne, P. Hyllus, D. Bruß, M. Lewenstein, and A. Sanpera, Phys. Rev. Lett. **92**, 087902 (2004).
 - [8] G. Tóth and O. Gühne, Phys. Rev. Lett. **94**, 060501 (2005).
 - [9] G. Tóth and O. Gühne, Phys. Rev. A **72**, 022340 (2005).
 - [10] Y. Tokunaga, S. Kuwashiro, T. Yamamoto, M. Koashi, and N. Imoto, Phys. Rev. Lett. **100**, 210501 (2008).
 - [11] W. Wieczorek, R. Krischek, N. Kiesel, P. Michelberger, G. Tóth, and H. Weinfurter, Phys. Rev. Lett. **103**, 020504 (2009).
 - [12] N. Kiesel, C. Schmid, U. Weber, G. Tóth, O. Gühne, R. Ursin, and H. Weinfurter, Phys. Rev. Lett. **95**, 210502 (2005).
 - [13] C.-Y. Lu, X.-Q. Zhou, O. Gühne, W.-B. Gao, J. Zhang, Z.-S. Yuan, A. Goebel, T. Yang, and J.-W. Pan, Nature Phys. **3**, 91 (2007).
 - [14] R. Ceccarelli, G. Vallone, F. De Martini, P. Mataloni, and A. Cabello, Phys. Rev. Lett. **103**, 160401 (2009).
 - [15] P. Walther, K. Resch, T. Rudolph, and et al., Nature **434**, 169 (2005).
 - [16] M. Weilenmann, B. Dive, D. Trillo, E. A. Aguilar, and M. Navascués, Phys. Rev. Lett. **124**, 200502 (2020).
 - [17] T. Das, S. S. Roy, S. Bagchi, A. Misra, A. Sen(De), and U. Sen, Phys. Rev. A **94**, 022336 (2016).
 - [18] A. Sen(De) and U. Sen, Phys. Rev. A **81**, 012308 (2010).
 - [19] X. Y. You Zhou, Qi Zhao and X. Ma, npj Quantum Information **5**, 83 (2019).
 - [20] O. Gühne and G. Tóth, Physics Reports **474**, 1–75 (2009).
 - [21] O. Gühne and N. Lütkenhaus, Phys. Rev. Lett. **96**, 170502 (2006).
 - [22] O. Gühne and N. Lütkenhaus, Journal of Physics: Conference Series **67**, 012004 (2007).
 - [23] J. M. Arrazola, O. Gittsovich, and N. Lütkenhaus, Phys. Rev. A **85**, 062327 (2012).
 - [24] T. Moroder, O. Gühne, and N. Lütkenhaus, Phys. Rev. A **78**, 032326 (2008).
 - [25] O. Gühne, P. Hyllus, D. Bruß, A. Ekert, M. Lewenstein, C. Macchiavello, and A. Sanpera, Phys. Rev. A **66**, 062305 (2002).
 - [26] O. Gühne and P. Hyllus, International Journal of Theoretical Physics **42**, 1001 (2003).
 - [27] K. Życzkowski and H.-J. Sommers, Journal of Physics A: Mathematical and General **36**, 10115 (2003).
 - [28] K. Życzkowski and H.-J. Sommers, Phys. Rev. A **71**, 032313 (2005).
 - [29] V. A. Osipov, H.-J. Sommers, and K. Życzkowski, Journal of Physics A: Mathematical and Theoretical **43**, 055302 (2010).
 - [30] O. Gühne, M. Reimpell, and R. F. Werner, Phys. Rev. Lett. **98**, 110502 (2007).
 - [31] J. Eisert, F. G. S. L. Brandão, and K. M. R. Audenaert, New Journal of Physics **9**, 46 (2007).
 - [32] M. B. Plenio and S. Virmani, “An introduction to entanglement measures,” (2005), arXiv:quant-ph/0504163 [quant-ph].
 - [33] M. B. Plenio and S. Virmani, Quantum Inf. Comput. **7**, 1 (2007).
 - [34] T.-C. Wei and P. M. Goldbart, Phys. Rev. A **68**, 042307 (2003).

- [35] P. Teng, Quantum Information Processing **16** (2017), 10.1007/s11128-017-1633-8.
- [36] A. Streltsov, H. Kampermann, and D. Bruß, Phys. Rev. A **84**, 022323 (2011).
- [37] H. J. Briegel and R. Raussendorf, Phys. Rev. Lett. **86**, 910 (2001).
- [38] R. Raussendorf and H. J. Briegel, Phys. Rev. Lett. **86**, 5188 (2001).
- [39] K. Chen, C.-M. Li, Q. Zhang, Y.-A. Chen, A. Goebel, S. Chen, A. Mair, and J.-W. Pan, Phys. Rev. Lett. **99**, 120503 (2007).
- [40] R. N. Alexander, P. Wang, N. Sridhar, M. Chen, O. Pfister, and N. C. Menicucci, Phys. Rev. A **94**, 032327 (2016).
- [41] D. L. Zhou, B. Zeng, Z. Xu, and C. P. Sun, Phys. Rev. A **68**, 062303 (2003).
- [42] H. Wunderlich, G. Vallone, P. Mataloni, and M. B. Plenio, New Journal of Physics **13**, 033033 (2011).
- [43] “Tucker decomposition — Wikipedia, the free encyclopedia,” (2020), [Online; accessed 12-July-2020].
- [44] T. G. Kolda and B. W. Bader, SIAM Review **51**, 455 (2009), <https://doi.org/10.1137/07070111X>.
- [45] B. W. Bader, T. G. Kolda, *et al.*, “Matlab tensor toolbox version 2.6,” Available online (2015).
- [46] L. V. Stephen Boyd, *Convex Optimization* (Cambridge University Press, 2004).
- [47] M.A.Nielson and I.L.Chuang, *Quantum Computation and Quantum Information* (Cambridge University Press, 2000).
- [48] S. Sciara, C. Reimer, M. Kues, P. Roztock, A. Cino, D. J. Moss, L. Caspani, W. J. Munro, and R. Morandotti, Phys. Rev. Lett. **122**, 120501 (2019).
- [49] M. Hein, J. Eisert, and H. J. Briegel, Phys. Rev. A **69**, 062311 (2004).
- [50] J. Eisert and H. J. Briegel, Phys. Rev. A **64**, 022306 (2001).

Appendix A: Numerical optimization algorithms

A simple optimization scheme for evaluating $\hat{E}_G(\mathcal{W})$ in Eq.(22) is introduced in Ref.[30]. Here we briefly summarize their scheme. If $|\phi\rangle$ is fixed, we can perform optimization by choosing $|\psi\rangle$ as the eigenvector corresponding to the largest eigenvalue of $(\mathcal{W} + |\phi\rangle\langle\phi|)$. If $|\psi\rangle$ is fixed, the way of finding the closest separable state is as follows: First we fix $|b\rangle, |c\rangle\dots$ and perform optimization on $|a\rangle$, then we fix $|a\rangle, |c\rangle\dots$ and perform optimization on $|b\rangle$. After several iterations we can arrive at the optimal separable state $|\phi\rangle$. Finally the optimization on $|\phi\rangle$ and $|\psi\rangle$ can be iterated, thus getting the value of $\hat{E}_G(\mathcal{W})$.

However, in numerical calculations we find the scheme above for finding optimal $|\phi\rangle$ often fail. In many cases

the iterations does not converge and get into an endless loop. We find the problem of numerically calculating the geometric entanglement(finding the optimal $|\phi\rangle$) was carefully studied before[35, 36]. Here we use the scheme introduced in [35].

The Tucker decomposition[43] of tensor $T_{mnp\dots z}$ is defined as

$$T_{mnp\dots z} = \sum \lambda_{\alpha\beta\gamma\dots\omega} a_{\alpha m} \circ a_{\beta n} \circ a_{\gamma p} \cdots \circ a_{\omega z} \quad (\text{A1})$$

The objective function of a rank-k approximation of the tensor $T_{mnp\dots z}$ can be written as

$$d = \min \left\| T_{mnp\dots z} - \sum_{i=1}^k \lambda_i a_{im} \circ a_{in} \cdots \circ a_{ip} \right\| \quad (\text{A2})$$

It is obvious that the problem of finding the separable state $|\phi\rangle$ with maximum overlap is same as finding the rank-1 approximation of tensor T. There are numerous algorithms that can be used for the rank-k approximation. The Alternate Least Squares algorithm is one of the most popular approaches. We will not discuss the details of the algorithms here. A complete survey of the algorithms can be found in Ref.[44]. There are also numerous existing code packages that can be utilized on different coding platforms, such as C++ or MATLAB etc. In this article, we use the MATLAB tensor toolbox 2.6 developed by Sandia National Laboratories[45]. This package is already developed and available online.

Hence, we can perform the optimization in Eq.(15) in the following way. By using the eigs function in MATLAB, we can compute the eigenvector $|\psi\rangle$ of $(\mathcal{W} + |\phi\rangle\langle\phi|)$ corresponding to the maximum eigenvalue. Then we fix $|\psi\rangle$ and compute the maximal overlapping separable state wave function $|\phi\rangle$ using the method introduced above. Then we do iteration of the two steps. The convergence of such iteration is very fast. In most cases, the numerical error can be reduced to less than 10^{-4} in less than 4 iterations.

After calculating $\hat{E}_G(\mathcal{W})$, the minimum value of c , we do optimization on the slope \vec{r} . As $\varepsilon(w)$ is a convex function of w , the Legend transformation $\hat{\varepsilon}(\vec{r})$ is also a convex function of \vec{r} [46]. So the Gradient Descent(GD) algorithm can be applied to perform optimization. For each iteration the slope \vec{r} is updated as

$$\vec{r} \rightarrow \vec{r} + \eta \nabla \hat{\varepsilon}(\vec{r}) \quad (\text{A3})$$

where η is the learning rate. After several iterations \vec{r} will reach the global maximum point of $\hat{\varepsilon}(\vec{r})$, which is the best lower bound of entanglement.